



Perfluorooctane sulfonate (PFOS) disrupts testosterone biosynthesis via CREB/CRTC2/StAR signaling pathway in Leydig cells

Lianglin Qiu^{a,*,1}, Hongxia Wang^{a,1}, Tianyi Dong^{a,1}, Jiyan Huang^a, Ting Li^a, Hang Ren^a, Xipei Wang^{a,c}, Jianhua Qu^a, Shoulin Wang^{b,**}

^a School of Public Health, Nantong University, 9 Sheyuan Rd., Nantong, 226019, PR China

^b Key Lab of Modern Toxicology of Ministry of Education, School of Public Health, Nanjing Medical University, 101 Longmian Avenue, Nanjing, 211166, PR China

^c Affiliated Haian Hospital of Nantong University, 17 Chengzhongbai Rd. Haian, Nantong, 226600, PR China

ARTICLE INFO

Keywords:

Perfluorooctane sulfonate (PFOS)
Steroidogenic acute regulatory protein
Testosterone biosynthesis
cAMP-response element binding protein
CREB regulated transcription coactivator 2
Protein kinase A
p38 Mitogen-activated protein kinase

ABSTRACT

Perfluorooctane sulfonate (PFOS), a stable end-product of perfluorinated compounds (PFCs), is associated with male reproductive disorders, but its underlying mechanisms are still unclear. We used in vivo and in vitro models to investigate the effects of PFOS on testosterone biosynthesis and related mechanisms. First, male ICR mice were orally administered PFOS (0–10 mg/kg/bw) for 4 weeks. Bodyweight, sperm count, reproductive hormones, mRNA expression of the genes related to testosterone biosynthesis, and the protein expression of protein kinase A (PKA), p38 mitogen-activated protein kinase (MAPK), cAMP-response element binding protein (CREB), CREB regulated transcription coactivator 2 (CRTC2) and steroidogenic acute regulatory protein (StAR) were evaluated. Furthermore, mouse primary Leydig cells were used to delineate the molecular mechanisms that mediate the effects of PFOS on testosterone biosynthesis. Our results demonstrated that PFOS dose-dependently decreased sperm count, testosterone level, CRTC2/StAR expression, and damaged testicular interstitium morphology, paralleled by increase in phosphorylated PKA, CREB and p38 in testes. Additionally, similar to the in vivo results, PFOS significantly decreased testosterone secretion, CRTC2/StAR expression, interaction between CREB and CRTC2 and binding of CREB/CRTC2 to StAR promoter region, paralleled by increase in phosphorylated-p38, PKA, and CREB expression. Meanwhile, inhibition of p38 by SB203580, or inhibition of PKA by H89 can significantly alleviate the above PFOS-induced effects. As such, the present study highlights a role of the CREB/CRTC2/StAR signaling pathway in PFOS-induced suppression of testosterone biosynthesis, advancing our understanding of molecular mechanisms for PFOS-induced male reproductive disorders

1. Introduction

Perfluorinated compounds (PFCs) are a class of synthetic fluorine-containing compounds widely used in many industrial and commercial products (Liu et al., 2020b). Due to the chemical, thermal stability, and bioaccumulation property, perfluorooctane sulfonate (PFOS), a stable end-product of PFCs, is known as a typical persistent organic pollutant (POP) and has relatively long elimination half-life in the body (Jian et al., 2017). In 2009, PFOS was listed in the Annex B of Stockholm Convention listings by United Nations Environment Programme (UNEP)

for the potential adverse effects on human health (UNEP, 2009). Whereafter, the precursor of PFOS, PFCs have been banned in the world gradually. However, PFOS has still been extensively detected in various biological samples. Therefore, the hazards of PFOS on the environment will continue for at least a few decades (Jian et al., 2017). Epidemiological evidence demonstrates that PFOS is associated with many human diseases such as thyroid disorder, deficit hyperactivity disorder, childhood obesity, type 2 diabetes and oligospermia (Ballesteros et al., 2017; Pan et al., 2019; Stratakis et al., 2020; Wang et al., 2015). Consistently, animal-based studies show that exposure to PFOS leads to neurotoxicity,

Abbreviations: PFOS, perfluorooctane sulfonate; PKA, protein kinase A; CREB, cAMP-response element binding protein; CRTC2, CREB regulated transcription coactivator 2; CRE, cAMP response element; StAR, steroidogenic acute regulatory protein.

* Corresponding author.

** Corresponding author at: School of Public Health, Nantong University, 9 Sheyuan Rd., Nantong, 226019, PR China.

E-mail addresses: llqiu@ntu.edu.cn (L. Qiu), wangshl@njmu.edu.cn (S. Wang).

¹ These authors contributed equally to this work.

<https://doi.org/10.1016/j.tox.2020.152663>

Received 18 September 2020; Received in revised form 29 November 2020; Accepted 15 December 2020

Available online 24 December 2020

0300-483X/© 2020 Elsevier B.V. All rights reserved.

hepatotoxicity, immunotoxicity and reproductive toxicity (Lindstrom et al., 2011; Mshaty et al., 2020; Wan et al., 2020).

Testosterone is central in the maintenance of male reproductive function (Salas-Huetos et al., 2020). Recently, both epidemiological and experimental studies confirm that exposure to PFOS leads to low testosterone levels in plasma (Joensen et al., 2013; Li et al., 2018a; Lopez-Doval et al., 2014). In testis, testosterone biosynthesis performs in Leydig cells, which depends on several important proteins such as steroidogenic acute regulatory protein (StAR/STARD1), cytochrome P450 CHOL side-chain cleavage enzyme (P450_{scc}), cytochrome P450 family 17a (CYP17a), 3 β -hydroxysteroid dehydrogenase (HSD3 β), 17 β -hydroxysteroid dehydrogenase (HSD17 β) and cytochrome P450 aromatase (P450_{arom}) (Zhou et al., 2019). StAR, one member of the START domain protein family, binds and facilitates cholesterol (CHOL) transfer from the outer to the inner mitochondrial membrane (Zirkin and Papadopoulos, 2018). With the help of STARD5, a directional cytosolic sterol transporter, and several enzymes (e.g. Cyp450_{scc}, Cyp450c17, HSD3 β , HSD17 β , and Cyp450_{arom}), testosterone biosynthesis is then initiated in Leydig cells (Zirkin and Papadopoulos, 2018). Growing evidence suggests that these proteins are susceptible to xenobiotics, especially endocrine disruptors (EDCs) (Huang et al., 2020; Xia et al., 2020). Interestingly, PFOS can disrupt thyroxine biosynthesis and be considered a typical EDC (Yu et al., 2009, 2011). Therefore, the process of testosterone biosynthesis and related regulatory proteins in Leydig cells may also be the targets for PFOS, which may contribute to PFOS-induced reproductive toxicity.

Cyclic AMP-response element-binding protein (CREB) and CREB regulated transcription coactivators (CRTC2s) are commonly known as the sensors for hormonal and metabolic signals, which involves in many pathophysiologic processes in drug-induced hepatitis, fatty liver disease and autoimmune disease (Altarejos and Montminy, 2011; Li et al., 2018b; Tout et al., 2018). Recent data suggests that CREB/CRTC2 works as the transcription coactivator and mediates StAR expression (Xu et al., 2014). Phosphorylation of CREB, recruitment of CREB binding protein, forming a complex with CRTC2, and binding to the StAR promoter are required during this process (Altarejos and Montminy, 2011). Interestingly, a recent study demonstrates that exposure to PFOS can increase phosphorylation of CREB and induce neurotoxic effects, suggesting that CREB may be an important molecular target for PFOS (Li et al., 2015). Therefore, considering the role of StAR in testosterone biosynthesis, we hypothesize that the CREB/CRTC2/StAR signaling pathway may involve in PFOS-induced disruption of testosterone and contribute to its reproductive toxicity.

In the present study, the *in vivo* and *in vitro* models were used to analyze the effects of PFOS on testicular histology, reproductive related hormones, mRNA expression of genes related to testosterone biosynthesis, protein expression of StAR and its upstream regulators, the interaction between CREB and CRTC2, and binding of CREB/CRTC2 to StAR promoter region. Our results showed that the exposure to PFOS significantly damaged the morphology of testicular interstitium and decreased testosterone secretion, CRTC2/StAR expression, interaction between CREB and CRTC2 and binding of CREB/CRTC2 complex to StAR promoter region, strongly supporting that PFOS disrupts testosterone biosynthesis by decreasing StAR via CREB/CRTC2 signaling pathway in Leydig Cells.

2. Method and materials

2.1. Chemicals and reagents

PFOS (purity \geq 98 %), Trypsin, collagenase, hyaluronidase and p-CREB antibody were purchased from Sigma-Aldrich Corp. (St. Louis, MO). Dulbecco's modified eagle's medium (DMEM) and fluorescent-labeled secondary antibodies (anti-rabbit IgG Alexa Fluor 488 and 555) were obtained from Thermo Fisher Scientific Inc. (Waltham, MA). The antibodies including p38, p-p38, CREB, StAR and glyceraldehyde-3-

phosphate dehydrogenase (GAPDH), anti-mouse IgG, anti-rabbit IgG, normal rabbit IgG and the inhibitors (H89 and SB203580) were purchased from Cell Signaling Technology Corp (Beverly, MA). The antibodies PKA and p-PKA were obtained from Abcam Corp. (Cambridge, MA). The CRTC2 antibody and the normal mouse IgG were purchased from Santa Cruz Corp. (Dallas, TX). All the other chemicals or reagents were the highest analytical grade.

2.2. Animal and treatment

Forty adult male ICR mice (7 weeks old, SLRC Laboratory Animal Company, Shanghai, China) were housed in a room with controlled temperature (25 \pm 1 °C) and 12 h/12 h light/ dark cycle. Mice were given free to access to drinking water and rat chow. The care and use of the animals during this experiment followed the guidelines of the Animal Care and Welfare Committee of Nantong University. After 1-week-adaptation, these mice (10 per group) were subjected to exposure to PFOS at the dose of 0.5, 5 and 10 mg/kg/bw by gavage for 4 weeks, which was conducted to simulate the high occupational exposure scenario (Lau et al., 2003; Wan et al., 2011; King et al., 2016). The control group was given the same volume of corn oil. All mouse euthanasia and tissue collection were performed on the day next to the last exposure.

2.3. Sperm count

Sperm count was conducted according to a previous report (Qiu et al., 2016). Briefly, the epididymes were quickly isolated from the PFOS- or vehicle treated mice and washed in normal saline. Then, the epididymis was weighted and placed in normal saline (1 mL). Six deep cuts were made in cauda with scissors to release sperm into medium. Next, the suspension was incubated at 35 °C for 10 min and then filtered with a 70- μ m nylon mesh. Finally, the suspension was stained with 0.25 % eosin Y (containing 0.5 % formalin) and counted by using a Neubaur counting chamber. The numbers of sperm were expressed as 10⁶/epididymis (g).

2.4. Testicular pathological analysis

The testicular pathological analysis was conducted according to a previous report (Qiu et al., 2018). Briefly, freshly isolated testes were fixed in 10 % formalin for 24 h. Then the testes were routinely dehydrated, embedded in paraffin, sliced (5- μ m thick) and subjected to hematoxylin and eosin staining.

2.5. Leydig cells isolation, culture and treatment

According to a previous report (Gao et al., 2020), primary Leydig cells were isolated from 4-week-old male ICR mouse testes. Briefly, freshly isolated testes were decapsulated and minced into pieces. After three washes, the seminiferous tubules were incubated with 20 mg/mL collagenase for 20 min at 37 °C with gentle shaking. Subsequently, cell suspension was filtered by a Nylon mesh (Pore size, 70 μ m). Leydig cells were then isolated by centrifugation (800 g \times 45 min) with percoll density gradient medium (GE Healthcare Life Sciences, Pittsburgh, PA). Purity of the cell preparations was verified by 3 β -hydroxysteroid dehydrogenase (3 β HSD) assay. Then, Leydig cells were maintained on plates with DMEM (containing 0.08 % serum albumin, 25 mM HEPES, 100 UI/mL penicillin and 50 μ g/mL streptomycin) and placed into a humidified CO₂ incubator at 37 °C with 5% CO₂ before stimulation.

For the *in vitro* experiments, primary Leydig cells were maintained in dishes and treated with PFOS (0, 15 and 30 mM) or DMSO (0.01 %). According to a previous report (Olsen et al., 2007), the serum PFOS concentration is found to be within the range of 0.25–12.83 μ g/mL (geometric mean: 2.44 μ g/mL) in occupational exposure workers. The levels are approximately equivalent to the dosage of PFOS range from 0.5 to 15 μ m, which is commonly used in the *in vitro* studies (Berntsen

et al., 2020; Liu et al., 2020a; Pham et al., 2020; Pierozan et al., 2020). In addition, the cytotoxicity test showed no significant toxic effects observed on Leydig cells treated with 30 μm of PFOS for 24 h (data not shown), which is conducted to ensure the effects of PFOS on Leydig cells are not due to cytotoxicity. Therefore, in the *in vitro* study, the highest dose of PFOS has been set at 30 μm , which is about 2 folds of the serum PFOS level in occupational exposure workers. The lower dose 15 μm is used to simulate the occupational exposure levels.

2.6. Enzyme-linked immunosorbent assay

According to a previous report (Qiu et al., 2018), reproductive related hormones including LH, FSH, testosterone (T), and estradiol (E2) in samples were measured using commercially available enzyme-linked immunosorbent assay (ELISA) kits (LH, CSB-E12770 m, CUSABIO, Maryland; FSH, LH-E10075MU, LIUHEBIO, Wuhan, China; T, IB79174, Minnesota; E2, ES180S-100, CALBIOTECH, California) according to the manufacturer directions. The sensitivities of the assay were 0.5 mIU/mL for LH, 0.064 mIU/mL for FSH, 0.066 ng/mL for T and 10 pg/mL for E2, respectively. The inter and intra experiment coefficients of variation were <15 % for LH, 5% for FSH, 6.5 % and 11.3 % for T, and 5% for E2, respectively. No replicates were used for the assessments of reproductive hormones in serum and testicular samples (n = 10 per group) due to the limited amount of each sample.

2.7. Real-time PCR

Primers in this study were designed using Primer Premier 5.0 software based on GenBank sequence of target genes including StAR (Forward Primer: 5'-ATGTTCTCGCTACGTTCAAG-3'; Reverse Primer: 5'-CCCAGTGCTCTCCAGTTGAG-3'), P450scc (Forward Primer: 5'-AGGTCCTTCAATGAGATCCCTT-3'; Reverse Primer: 5'-TCCCTGTAAATGGGGCCATAC-3'), CYP17a (Forward Primer: 5'-GCCCAAGTCAAAGACACCTAAT-3'; Reverse Primer: 5'-GTACC-CAGGCGAAGAGAATAG-3'), HSD3b (Forward Primer: 5'-CCTCCGCCTTGATACCAGC-3'; Reverse Primer: 5'-TTGTTCCAATCTCCCTGTGC-3'), HSD17b (Forward Primer: 5'-ACTTGGCTGTTCGCCTAGC-3'; Reverse Primer: 5'-GAGGGCATCCTTGAGTCTG-3'), P450arom (Forward Primer: 5'-ATGTTCTTGGAAATGCTGAACCC-3'; Reverse Primer: 5'-AGGACCTGGTATTGAAGACGAG-3) and GAPDH (Forward Primer: 5'-TGAACGGGAAGCTCACTGG-3'; Reverse Primer: 5'-TCCAC-CACCTGTGCTGTA-3') and synthesized by Genaray Biotechnology (Shanghai, China). Total RNA was isolated from the mouse testes or primary Leydig cells using TRIzol (Invitrogen, Carlsbad, CA) and converted to cDNA using a Revert Aid First Stand cDNA Synthesis Kit (Fermentas, Vilnius, Lithuania). Quantitative polymerase chain reaction (qPCR) was performed using a FastStart Universal SYBR Green Master (ROX) system (Roche, Indianapolis, Indiana) and Lightcycler 480 (Roche, Mannheim, Germany) (Qiu et al., 2018). All qPCRs were performed in triplicate, and the specificity of the PCR products was confirmed using melting curve analyses. Relative gene expression levels, normalized to GAPDH expression, were calculated as $2^{-\Delta\Delta Ct}$. Gene expression levels in the treatment group are expressed as a percentage compared with the control groups.

2.8. Immunoblot analysis

The immunoblot analysis was performed according to a previous report (Qiu et al., 2016). The fresh dissected testes and PFOS-treated Leydig cells were homogenized and lysed for 30 min in lysis buffer on ice. After sonication and centrifugation, the lysates (100 μg) were subjected to SDS-PAGE and transferred to PVDF membranes. Immune complexes were detected by enhanced chemiluminescence using specific antibodies including PKA, p-PKA, p38, p-p38, CREB, p-CREB, CRT2, StAR and glyceraldehyde-3-phosphate dehydrogenase. (For details, see Supplementary Material Table S1.) For the densitometric

analysis, the protein bands on the blots were measured using 1.45 s software (National Institutes of Health, USA).

2.9. Immunofluorescence analysis

Immunofluorescence analysis was conducted according to a previous report (Qiu et al., 2016). Briefly, for the testicular paraffin sections, they were incubated with goat serum (containing 0.5 % Triton X-100) followed by incubating with the primary antibody StAR at 4 °C overnight. For the primary Leydig cells, they were maintained in 35 mm glass dish and treated with PFOS (0, 15 and 30 mM) or DMSO (0.01 %). Then the cells were washed and fixed in acetone for 10 min. After washing, the cells were incubated with goat serum (containing 0.5 % Triton X-100) followed by incubating with the primary antibody StAR at 4 °C overnight. Then these samples were incubated with fluorescent-labeled secondary antibodies for 40 min at a dark place. The localization of these proteins in samples was detected by a fluorescence microscopy (Leica, Wetzlar, Germany).

2.10. Immunoprecipitation and chromatin immunoprecipitation assay

Immunoprecipitation were conducted as previously described (Qiu et al., 2016). Briefly, after treatment, Leydig cells were lysed on ice with the lysis buffer. The lysate was then incubated with anti-CRTC2 mouse monoclonal antibody in the presence of protein A/G agarose (Thermo Fisher Scientific, Waltham, MA) according to manufacturer's instructions. Normal mouse IgG was used as negative control. After washing, the samples were subjected to SDS-PAGE followed by immunoblot analysis with specific p-CREB and CREB antibodies. Chromatin immunoprecipitation (ChIP) was performed using a ChIP assay kit (Thermo Fisher Scientific, Rockford, IL) according to the manufacturer's instructions (Lai et al., 2014). Briefly, cells were cross-linked by 1% formaldehyde for 10 min at 25 °C and harvested in ice-cold PBS containing 1% Halt Cocktail (Thermo Fisher Scientific, Rockford, IL). The cross-linked cells were then lysed and followed by incubation with micrococcal nuclease (10U/ μl) to shear genomic DNA. The antibodies CRTC2 and CREB, and rabbit IgG (Cell Signaling Technology, Beverly, MA) were used for immunoprecipitation. After washing, Protein/DNA complexes were eluted from the beads and then incubated with proteinase K solution at 65 °C for 2.5 h. After purification, DNA samples were used as templates to amplify the StAR promoter region by Real-time PCR with the primers 5'-TAAAAGCGCTGGTGACACAC-3' and 5'-CCGTCTAGCCTTCAAACAGC-3'. Primers spanning the three CRE sites at -305 bp to -75 bp of the StAR promoter. The real-time PCR ChIP results were analyzed using $\Delta\Delta Ct$ method (Xu et al., 2014). Briefly, each ChIP DNA fractions' Ct value was normalized to the input DNA fraction Ct value for the same qPCR Assay (ΔCt) to account for chromatin sample preparation differences using the formula: $\Delta Ct_{(\text{normalized ChIP})} = Ct_{(\text{ChIP})} - [Ct_{(\text{input})} - \log_2(\text{input dilution factor})]$. Then, the difference between the ChIP fraction Ct values ($\Delta\Delta Ct$) of the normalized experimental sample (S2) and the control sample (S1) was determined using the formula: $\Delta\Delta Ct_{(S2-S1)} = \Delta Ct_{(S2:\text{normalized ChIP})} - \Delta Ct_{(S1:\text{normalized ChIP})}$. Next, the differential occupancy fold change (linear conversion of the second $\Delta\Delta Ct$ to yield a fold change in site occupancy) determined using the formula: $\text{Fold Change in Occupancy} = 2^{[-\Delta\Delta Ct_{(S2-S1)}]}$. Finally, q-PCR products were further subjected to electrophoresis in 2% agarose for analysis.

2.11. Statistical analysis

In this study, the SPSS 17.0 software (SPSS, Inc., Chicago, IL) for Windows was used to analyze the quantitative data by one-way analysis of variance (ANOVA) and Duncan's post hoc test. The level for statistical significance was set at $p < 0.05$.

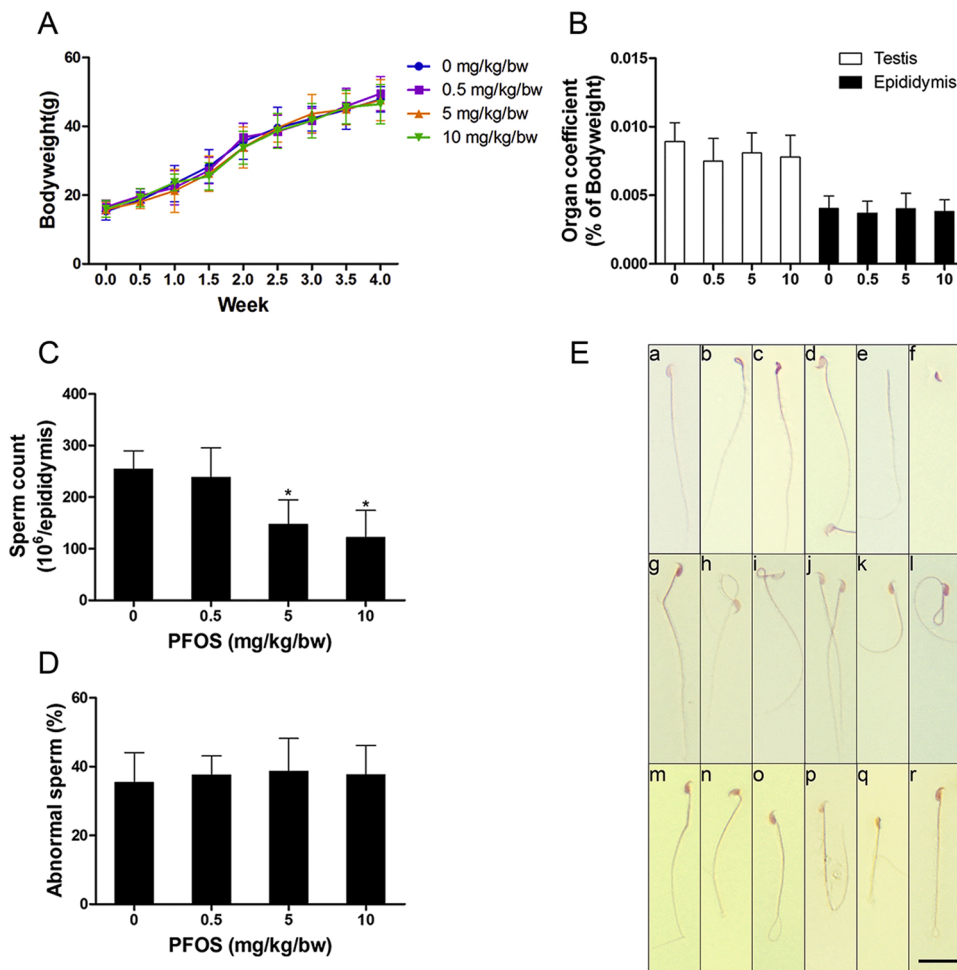


Fig. 1. The effects of PFOS exposure on mice bodyweight and sexual gland. Mice were orally administrated PFOS (0–10 mg/kg/bw) by gavage for 4 weeks. The control group was given the same volume of corn oil. Mice bodyweights were monitored twice a week during the exposure period. A. Bodyweight. B. Organ coefficient of testes and epididymis. After exposure, testes and epididymis were isolated and weighted, and normalized to the bodyweight. C. Sperm count. D. Abnormal sperm rate. E. Abnormal sperm morphology. a: normal sperm; b-f: Abnormal sperm head; g-l: Abnormal sperm neck; m-n: Abnormal sperm tail. Sperm was stained with 0.25 % eosin Y and counted by using a Neubaur's counting chamber. The numbers of sperm were expressed as 10^6 /epididymis weight (g). Scale bar: 10 μ m.

3. Results

3.1. Exposure to PFOS reduces the sperm count in epididymis

To examine the effects of exposure to PFOS on the male reproductive system, we exposed male ICR mice to PFOS at the doses range from 0 to 10 mg/kg by oral for 4 weeks. Fig. 1A and B demonstrate that this exposure to PFOS did not significantly change the bodyweights or the organ coefficient of testes and epididymis of mice. However, exposure to PFOS significantly decreased the sperm count in epididymis (Fig. 1C) without changes in abnormal sperm rate (Fig. 1D and E).

3.2. Exposure to PFOS decreases the testicular and circulating testosterone levels, and alters mice testicular histology

Reproductive hormones are central in the maintenance of spermatogenesis (Zirkin and Papadopoulos, 2018). To delineate the possible mechanism whereby exposure to PFOS decreases sperm count in the epididymis, the testicular and serum samples from these vehicle- or PFOS-treated mice were subjected to analysis of reproductive hormone levels. Fig. 2Aa reveals that exposure to PFOS significantly decreased serum testosterone levels. In contrast, it did not significantly alter serum estradiol, FSH and LH levels (Fig. 2Ab–Ad). Consistent with its effects in serum, exposure to PFOS reduced testicular testosterone levels (Fig. 2Ae) without changes in testicular estradiol, FSH and LH levels (Fig. 2Af–Ah). To further verify the changes in testicular testosterone levels, the testes from vehicle- or PFOS-treated mice were subjected to pathological assessments. Although no any significant abnormality in

the structure and morphology of testicular interstitium was observed in vehicle- treated controls (Fig. 2Ba and Be), we observed a significant increase in Leydig cell vacuolization in PFOS-treated mice at dose of 5 mg/kg/bw and higher (Fig. 2Bc, Bd, Bg and Bh), and degeneration of germ cells in seminiferous epithelium in PFOS-treated groups at dose of 10 mg/kg/bw (Fig. 2Bd and Bh).

3.3. Exposure to PFOS alters the testicular expression of genes related to testosterone biosynthesis

In male genital gland, several genes, StAR, P450scc, P450c17, HSD3 β , HSD17 β and P450arom, are critical for testosterone biosynthesis (Zirkin and Papadopoulos, 2018). To determine how PFOS reduces testosterone biosynthesis, we assessed the mRNA expression of StAR, P450scc, P450c17, HSD3 β , HSD17 β and P450arom in testes. As shown in Fig. 3, exposure to PFOS significantly decreased the testicular mRNA level of StAR (Fig. 3A), but not P450scc, P450c17, HSD3 β , HSD17 β and P450arom (Fig. 3B–F)

3.4. Exposure to PFOS alters the testicular expression of StAR and its upstream regulating factors

To determine how PFOS reduces testicular StAR expression, we analyzed the protein expression of StAR and its upstream regulators (CRT2, CREB, p-CREB, p38, p-p38, PKA and p-PKA) in testes. Fig. 4A demonstrates that exposure to PFOS significantly increased the protein expression of p-PKA, p-p38, and p-CREB (especially at dose of 5 mg/kg/bw and higher) in mice testes. In contrast, CRT2 and StAR were

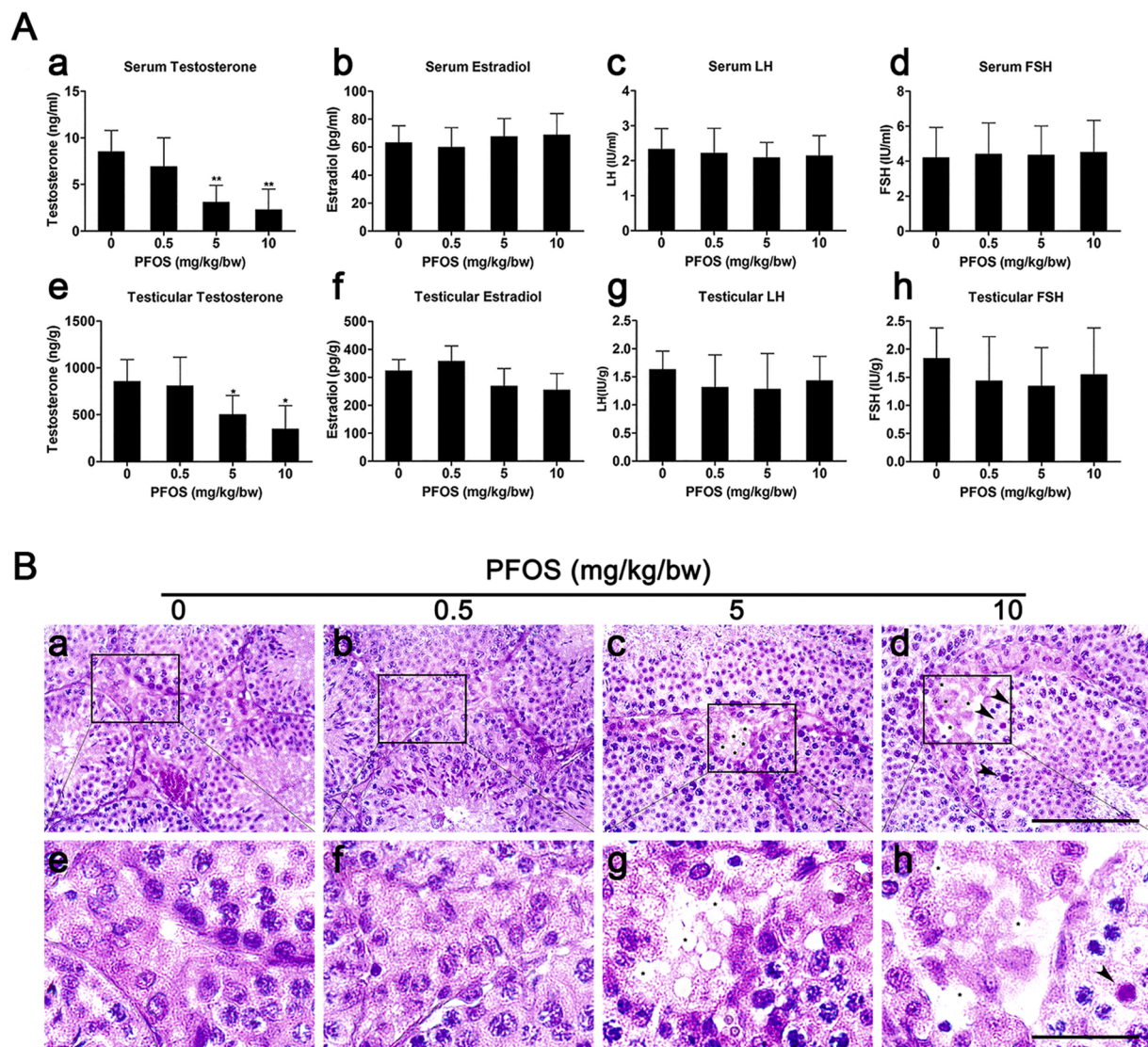


Fig. 2. The effects of PFOS exposure on testicular interstitium histology and reproductive related hormones.

Mice were orally administered PFOS (0–10 mg/kg/bw) by gavage for 4 weeks. The control group was given the same volume of corn oil. A. The level of reproductive related hormones. a. Serum testosterone; b. Serum estradiol; c. Serum LH; d. Serum FSH; e. Testicular testosterone; f. Testicular estradiol; g. Testicular LH; h. Testicular FSH. The data are expressed as the mean \pm SD, $n = 10$ per group. * $p < 0.05$, ** $p < 0.01$ compared with control group. B. a–d: The testicular interstitium morphology of mice; e–h: The magnification images of the selected area from a–d. Black arrow head: immature germ cells. Asterisk: Leydig cell vacuolization. $n = 10$ per group. Bar in the upper panel: 100 μm . Bar in the lower panel: 20 μm .

markedly decreased at these PFOS-exposed mice. To further confirm the changes in StAR expression, the testicular sections from vehicle- or PFOS-treated mice were subjected to immunofluorescent staining. Fig. 4B demonstrate that exposure to PFOS significantly decreased the testicular StAR expression.

3.5. Exposure to PFOS alters the testosterone secretion and StAR mRNA expression in Leydig cells

To verify the *in vivo* results, we exposed primary Leydig cells to PFOS and assessed the testosterone secretion and the mRNA expression of genes (StAR, P450scc, P450c17, HSD3 β , HSD17 β and P450arom) in Leydig cells. Fig. 5A demonstrates that exposure to PFOS significantly decreased the secretion of testosterone in Leydig cell and expression of StAR in Leydig cells. In parallel to the changes of testosterone secretion, PFOS significantly decreased mRNA expression of StAR but not P450scc, P450c17, HSD3 β , HSD17 β and P450arom (Fig. 5B).

3.6. Exposure to PFOS alters the protein expression of StAR and its upstream regulators in Leydig cells

To delineate the molecular mechanisms whereby exposure to PFOS reduces StAR expression, we exposed primary Leydig cells to PFOS and assessed the protein expression of StAR and its upstream regulators (PKA, p-PKA, p38, p-p38, CREB, p-CREB and CRTC2) in Leydig cells. Fig. 6A shows that PFOS dose-dependently increased protein expression of p-PKA, p-p38 and p-CREB in Leydig cells. In contrast, exposure to PFOS significantly decreased the protein expression of StAR and CRTC2 (Fig. 6A and B) in Leydig cells. There were no markedly changes in the expression of PKA, p38 and CREB in Leydig cells (Fig. 6A).

3.7. Exposure to PFOS decrease the interaction between CREB and CRTC2

To test if PFOS exposure impacts the interaction between CREB and its coactivator CRTC2, we exposed Leydig cells to PFOS and assessed the

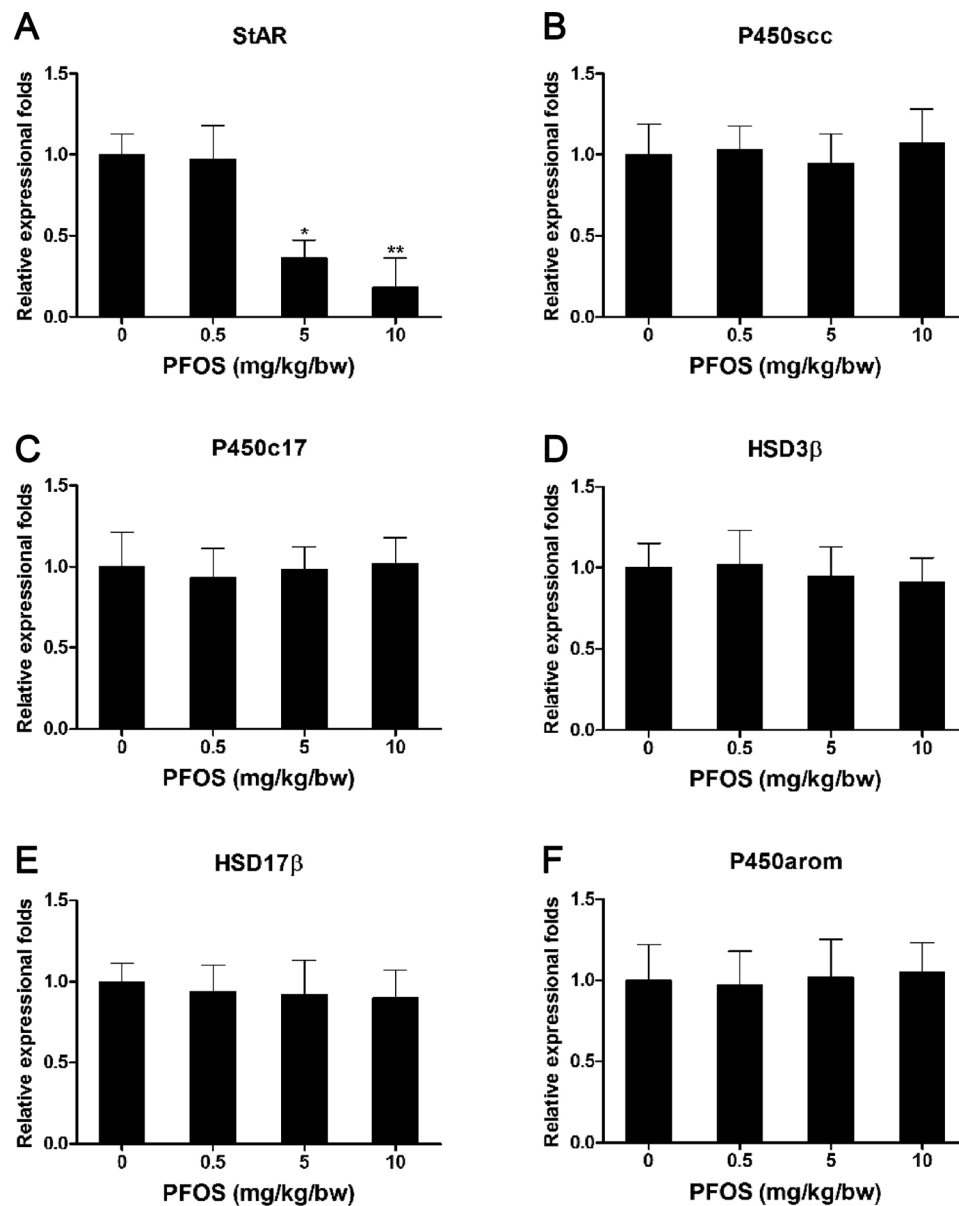


Fig. 3. The effects of PFOS exposure on mRNA expression of genes related to testosterone biosynthesis. Mice were orally administrated PFOS (0–10 mg/kg/bw) by gavage for 4 weeks. The control group was given the same volume of corn oil. A. StAR; B. P450scc; C. P450c17; D. HSD3β; E. HSD17β; F. P450arom. The data are expressed as the mean \pm SD, n = 10 per group. *p < 0.05, **p < 0.01, compared with control group.

interaction between CREB and CRTC2 using a co-immunoprecipitation assay. Fig. 6C demonstrates that exposure to PFOS significantly decreased the interaction between p-CREB (the activated form of CREB)/CREB and CRTC2. To further document the effects of PFOS exposure on the binding of CREB/CRTC2 complex to the StAR promoter region, Leydig cells were exposed to PFOS and then subjected to a chromatin immunoprecipitation assay. As shown in Fig. 6D, exposure to PFOS decreased the binding of CREB/CRTC2 complex to the StAR promoter region.

3.8. Inhibitor H89 or SB203580 attenuates PFOS-induced decrease in StAR expression and testosterone secretion in Leydig cells

Protein kinase A (PKA) and p38 MAPK signaling pathways have been reported to activate CREB and its co-activator CRTC2, suggesting that they may also involve in the expression regulation of StAR gene (Lee et al., 2015; Tugaeva and Sluchanko, 2019; Xu et al., 2014). CREB/CRTC2 can bind to StAR promoter region and initiate StAR

expression. Therefore, to delineate the mechanisms whereby exposure to PFOS decreases StAR expression, the lysates from these PFOS-exposed Leydig cells treatment with or without the inhibitors (H89, a specific inhibitor for PKA, or SB203580, a specific inhibitor for p38) were subjected to immunoblot analysis. As shown in Fig. 7A, exposure to PFOS significantly increased the protein expression of p-PKA, p-p38 and p-CREB while decreased that of CRTC2 and StAR in Leydig cells, which were significantly alleviated by treatment with inhibitors, H89 and SB203580. Fig. 7B reveals that the inhibitors, H89 and SB203580, markedly assuaged PFOS-induced decrease in StAR expression in Leydig cells. Fig. 7C demonstrates that PFOS-induced decrease in the interaction between CREB and CRTC2 was attenuated by the inhibitors, H89 and SB203580. Similarly, H89 or SB203580 significantly rescued the PFOS-induced decrease in binding of CREB/CRTC2 complex to the StAR promoter region (Fig. 7D). To further confirm the above results, we exposed primary Leydig cells to PFOS with or without the inhibitors (H89 and SB203580) and evaluated the testosterone secretion in Leydig cells. In parallel to the changes of StAR expression, PFOS-induced the

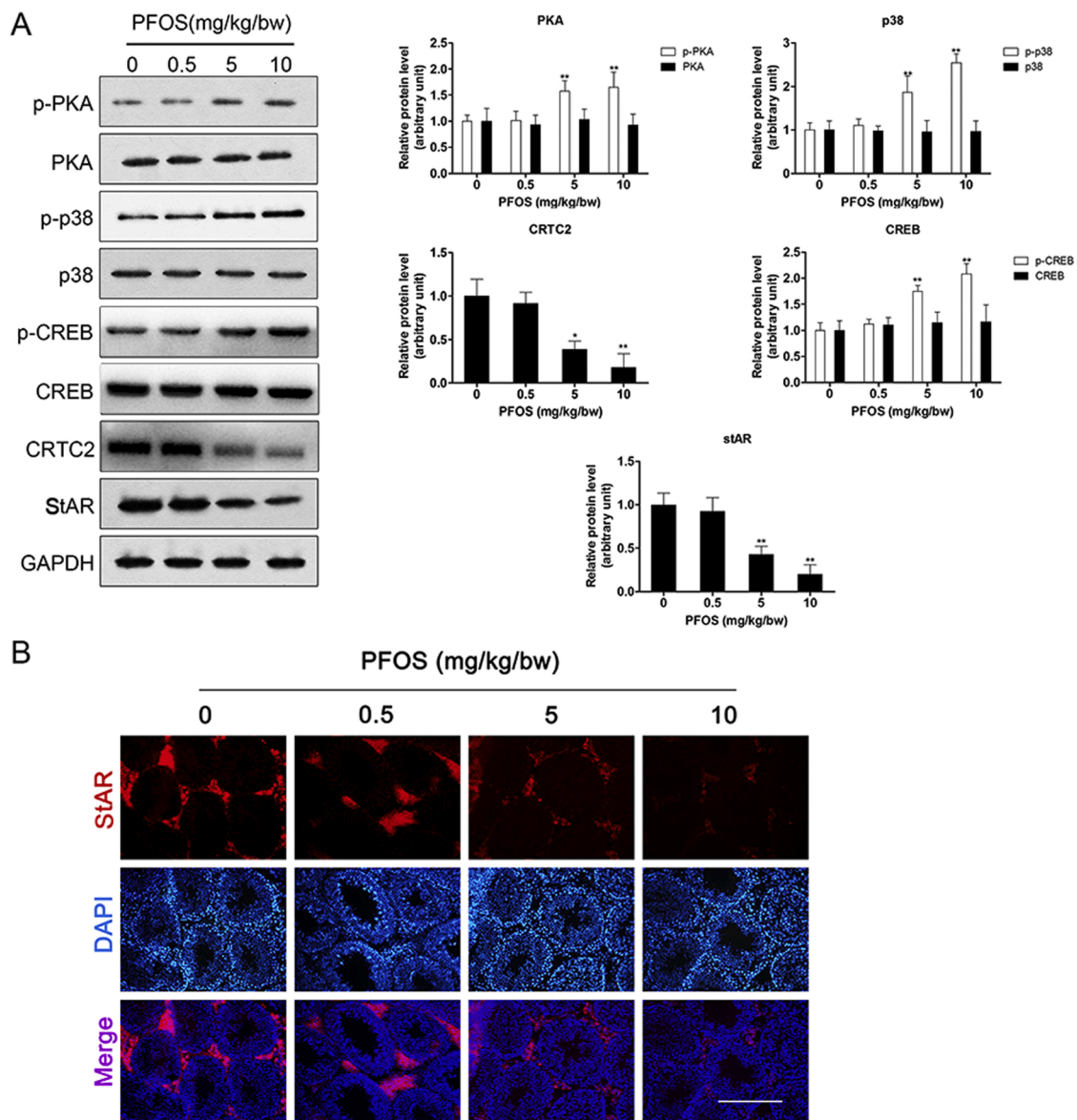


Fig. 4. The effects of PFOS exposure on protein expression of StAR and its upstream regulators in testis. Mice were orally administrated PFOS (0–10 mg/kg/bw) by gavage for 4 weeks. The control group was given the same volume of corn oil. **A.** The protein expression of StAR and its upstream regulators in testis. The protein expression was determined using immunoblot assay and the densitometric analysis was conducted for the protein bands using ImageJ software. Each value was normalized to Glyceraldehyde-3-phosphate dehydrogenase (an internal reference), and the relative expression levels were generated compared with the control value. The data are expressed as the mean \pm SD, $n = 10$ per group. * $p < 0.05$, ** $p < 0.01$, compared with control group. **B.** The localization of StAR protein in testis detected by immunofluorometric assay. StAR (red), Cell nucleus (blue); Scale bar: 100 μ m.

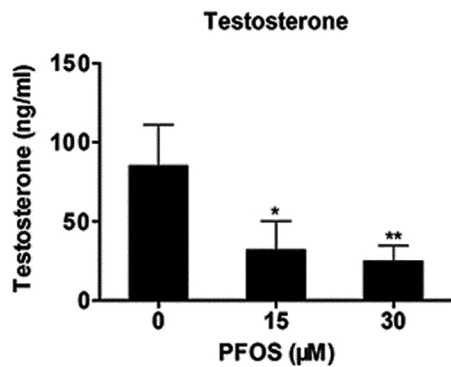
suppression of testosterone secretion was also markedly attenuated by these inhibitors (Fig. 7E).

4. Discussion

Growing evidence indicates that male reproductive system is susceptible to environmental pollutants (Sifakis et al., 2017). Perfluorooctane sulfonate, a stable end-product of PFCs, is a typical environmental pollutant and associated with male reproductive disorder (Pan et al., 2019). However, its related toxic mechanisms on male reproductive system are still unclear. In the present study, we systemically examined the effects of PFOS on the murine male reproductive system. In this study, mice were exposed to PFOS at the dose range of 0.5–10 mg/kg/bw for 4 weeks according to the previous report (Wan et al., 2011), which was conducted to simulate the high occupational exposure scenario. Reportedly, the serum PFOS concentration is found

to be within range of 0.25–12.83 μ g/mL (geometric mean: 2.44 μ g/mL) in occupational exposure workers, which is approximately 1000-fold higher than that in general public (geometric mean: 2.07 ng/mL) (Olsen et al., 2007), suggesting that occupational exposure workers may have relatively higher health risks than the latter. Therefore, in this study, the highest dose has been set at 10 mg/kg/bw to simulate the equivalent dose of exposure for occupational exposure workers. The lowest dose 0.5 mg/kg/bw has been determined according to the reported No-observed-adverse-effect-level (NOAEL) for PFOS in mouse (Dong et al., 2009). The entire spermatogenic process takes approximately 28 days in a mouse (Ray et al. 2014). Therefore, in this study, mice were exposed for 4 weeks, which is to cover the cycle of spermatogenesis. The main findings include that 1) exposure to PFOS significantly damaged the structure and morphology of testicular interstitium in testes, which was paralleled by decreases in testicular and circulating testosterone level; 2) exposure to PFOS significantly

A



B

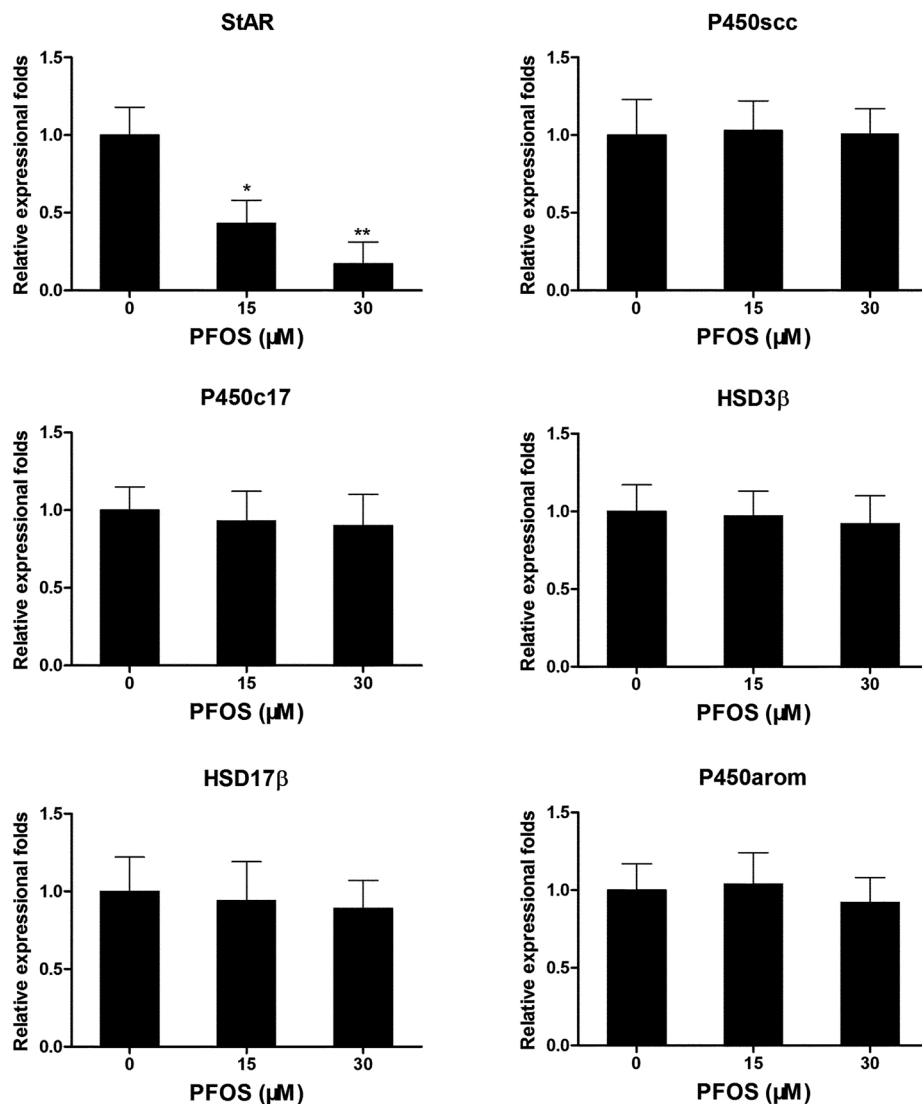


Fig. 5. The effects of PFOS exposure on testosterone secretion and mRNA expression of genes related to testosterone biosynthesis in Leydig cells.

Primary Leydig cells (1×10^7 cells) were seeded in Matrigel-coated 100-mm dish and incubated for 24 h. Then, the cells were treated with PFOS (0–30 μM) for 24 h. The medium was collected for analysis of testosterone secretion. Leydig cells were harvested for quantitative analysis of mRNA expression of genes related to testosterone biosynthesis. A. The testosterone level in the medium from vehicle- or PFOS-treated group. B. The mRNA expression of genes related to testosterone biosynthesis in Leydig cells. The data are expressed as the mean \pm SD, $n = 6$ per group. * $p < 0.05$, ** $p < 0.01$, compared with control group.

decreased mRNA/protein levels of StAR gene in testes, which was accompanied by increases in the protein level of its upstream regulators: p-PKA, p-p38 and p-CREB; 3) exposure to PFOS significantly decreased protein levels of CRTC2, a co-actor of CREB, in testes; 4) the changes in CRTC2 were paralleled by decrease in interaction between CRTC2 and CREB and binding of CREB/CRTC2 to StAR promoter region; 5) inhibition of p38 MAPK or PKA signaling pathway significantly alleviated the above changes in Leydig cells; 6) meanwhile, PFOS-induced decreases in StAR expression and testosterone secretion in Leydig cells

were also recovered by inhibition of these two signaling pathway. These data collectively suggest that exposure to PFOS may disrupt testosterone biosynthesis via CREB/CRTC2/StAR signaling pathway.

Epidemiological evidence shows that PFOS is negatively associated with circulating testosterone levels suggesting that PFOS may affect testosterone biosynthesis in testis (Pan et al., 2019). Testicular pathology is one of the most critical indicators to evaluate the male reproductive injury. The present data have demonstrated that exposure to PFOS remarkably damaged testicular interstitium structure and

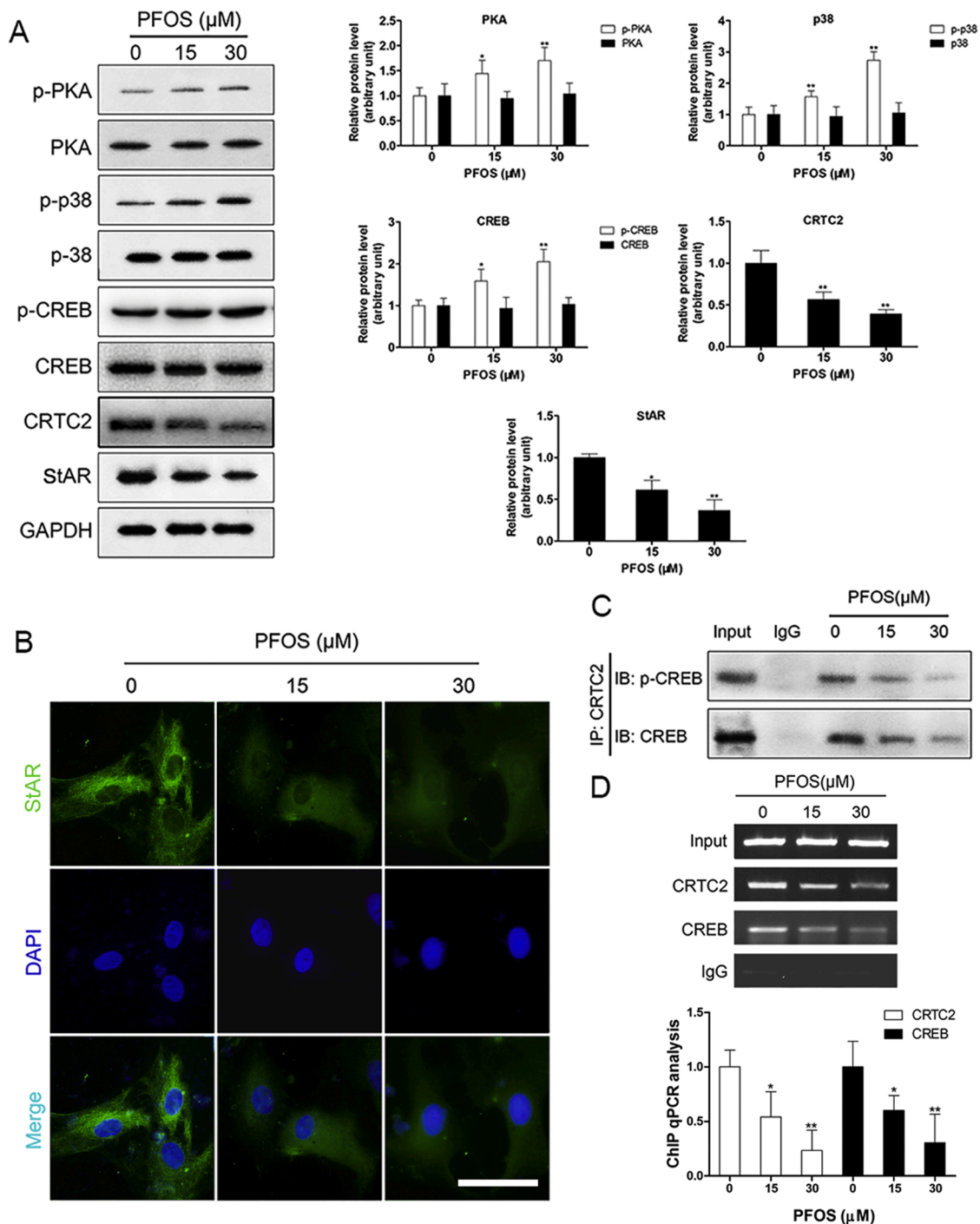


Fig. 6. The effects of PFOS exposure on the regulation of StAR gene expression in Leydig cells. Primary Leydig cells (1×10^7 cells) were seeded in Matrigel-coated 100-mm dishes and incubated for 24 h. Then, the cells were treated with PFOS (0–30 μM) for 24 h. A. The protein expression of StAR and its upstream regulators. The protein expression was determined using immunoblot assay and the densitometric analysis was conducted for the protein bands using ImageJ software. Glyceraldehyde-3-phosphate dehydrogenase was employed as an internal reference. The data are expressed as the mean \pm SD, $n = 6$ per group. * $p < 0.05$, ** $p < 0.01$, compared with control group. B. The localization of StAR protein in Leydig cells. StAR (green), Cell nucleus (blue); Scale bar: 20 μm. C. After treatment with PFOS or vehicle, the cells were homogenized and immunoprecipitated with anti-CRTC2 antibody. The total/phosphorylated CREB expression was analyzed by immunoblot assay. D. After treatment with PFOS or vehicle, Leydig cells were cross-linked with formaldehyde and lysed. The precleared chromatin was immunoprecipitated with anti-CRTC2, anti-CREB or normal rabbit IgG antibodies. The binding of CRTC2/CREB to the StAR promoter region was analyzed by Q-PCR using the StAR promoter primers. The qPCR products were then analyzed by agarose gel electrophoresis assay. The data are expressed as the mean \pm SD, $n = 6$ per group. * $p < 0.05$, ** $p < 0.01$, compared with control group.

morphology, paralleled by a decrease in testicular and circulating testosterone levels. This is consistent with previous studies showing that orally exposure to PFOS significantly decreases testosterone levels in rats (Li et al., 2018a; Lopez-Doval et al., 2014). Therefore, these data

suggest that PFOS-induced decrease in testosterone levels may be attributable to the damage in testicular interstitium's structure and function.

Biosynthesis of testosterone is a vital function of the testicular

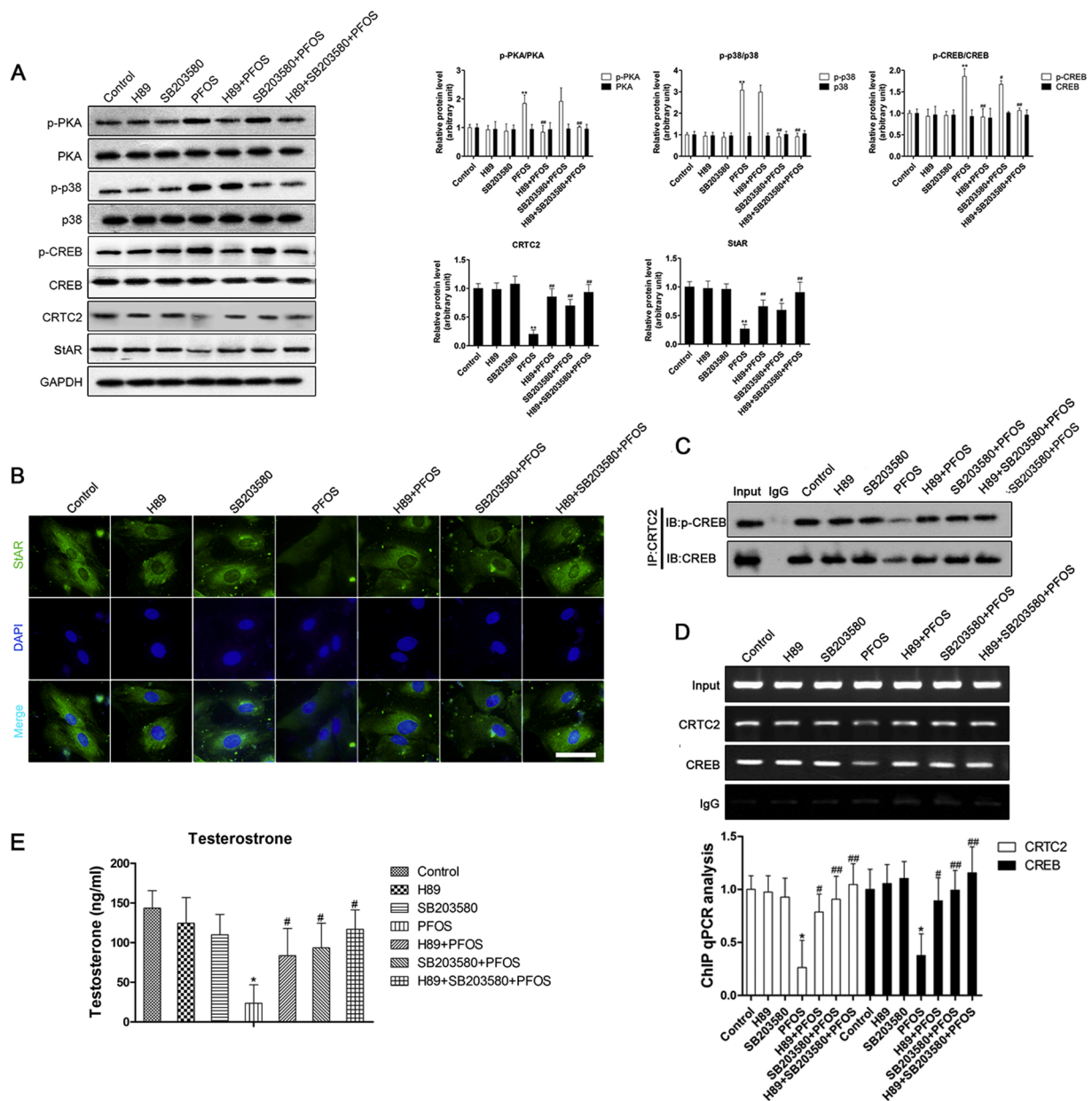


Fig. 7. The effects of PFOS and inhibitors (H89 or SB203580) on the regulation of StAR gene expression in Leydig cells. Primary Leydig cells (1×10^7 cells) were seeded in Matrigel-coated 100-mm dishes and incubated for 24 h. The cells were then pretreated with the inhibitors (10 μ M H89 or 10 μ M SB203580) and further incubated with PFOS (30 μ M) for 24 h. **A.** The protein expression of StAR and its upstream regulators were analyzed by immunoblot assay. The data are expressed as the mean \pm SD, $n = 6$ per group. * $p < 0.05$, ** $p < 0.01$, compared with control group; # $p < 0.05$, ## $p < 0.01$, compared with PFOS-treated group. **B.** The localization of StAR protein in Leydig cells testis was detected by immunofluorometric assay. StAR (green), Cell nucleus (blue); Scale bar: 20 μ m. **C.** After treatment, the cells were homogenized and immunoprecipitated with anti-CRTC2 antibody. The total/phosphorylated CREB expressions were analyzed by immunoblot assay. **D.** After treatment, Leydig cells were cross-linked with formaldehyde and lysed. The precleared chromatin was immunoprecipitated with anti-CRTC2, anti-CREB or normal rabbit IgG antibodies. The binding of CRTC2/CREB to the StAR promoter region was analyzed by Q-PCR using the StAR promoter primers. The qPCR products were then analyzed by agarose gel electrophoresis assay. The data are expressed as the mean \pm SD, $n = 6$ per group. * $p < 0.05$, ** $p < 0.01$, compared with control group.

interstitium, which is critical for maintaining normal male reproductive functions (Zirkin and Papadopoulos 2018). Biosynthesis of testosterone is primarily regulated by the proteins, such as StAR, P450_{scc}, P450_{c17}, HSD3 β , HSD17 β and P450_{arom}, related to steroid metabolism (Zirkin and Papadopoulos, 2018). Another important finding in the present study is that exposure to PFOS remarkably decreased StAR expression in testes. StAR can carry CHOL from the outer to the inner mitochondrial membrane and initiate testosterone biosynthesis (Tugaeva and Sluchanko, 2019). Therefore, this data not only consolidates the finding that exposure to PFOS decreases testicular and circulating testosterone

levels but also strongly suggests that this reduction of testosterone levels may be attributable to the decrease in StAR expression in testes.

Current research on CREB/CRTC2/StAR signaling pathway focuses on its role in metabolic diseases (Altarejos and Montminy, 2011; Delghandi et al., 2005). CREB and CRTC2 are the sensors for hormonal and metabolic signals, contributing to glycometabolism and lipid metabolism (Altarejos and Montminy, 2011). Interestingly, recent research shows that the CREB/CRTC2 signaling pathway also responds to the stimulus signal of xenobiotics (Altarejos and Montminy, 2011). Interestingly, recent research shows that CREB/CRTC2 signaling pathway

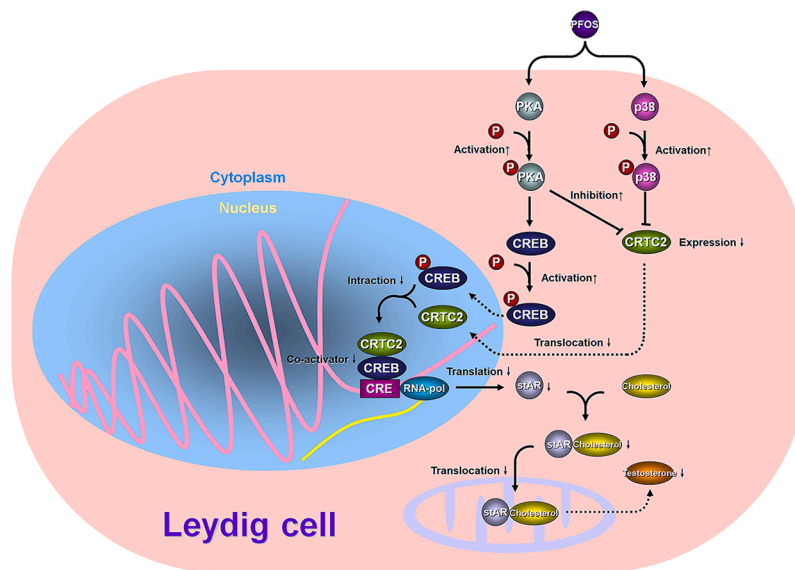


Fig. 8. A schematic diagram of the proposed mechanisms of CREB/CRTC2/StAR signaling pathway mediating PFOS-induced suppression of testosterone biosynthesis. P: phosphate; PFOS: perfluorooctane sulfonate; PKA: protein kinase A; CREB: cAMP-response element binding protein; CRTC2: CREB regulated transcription coactivator 2; CRE: cAMP response element; StAR: steroidogenic acute regulatory protein.

also responds to the stimulus signal of xenobiotics (Xu et al., 2014). In the present study, we have found that exposure to PFOS significantly decreased the protein expression of CRTC2 and StAR in testes. Noticeably, CREB/CRTC2 works as the transcription co-activator and is involved in regulating StAR gene expression (Tugaeva and Sluchanko, 2019). Therefore, the decrease in CRTC2 expression may contribute to PFOS-induced reduction in StAR gene expression. To further verify the above hypothesis, the expressions of CREB/CRTC2, PKA and p38 MAPK signaling pathways in mice testes were analyzed. PKA is a crucial upstream regulator of the CREB/CRTC2 signaling pathway, and p38 MAPK is a critical signal transduction molecule for PFOS-induced toxic effects (Moon et al., 2016; Qiu et al., 2016). Our data show that exposure to PFOS significantly increased phosphorylation of PKA and p38, paralleled by the decrease of CRTC2/StAR expression in testes, suggesting that these upstream regulators of CREB/CRTC2 signaling pathway may also involve in regulating the expression of StAR. Similarly, the in vitro data shows that exposure to PFOS significantly decreased the CRTC2/StAR expression and suppressed testosterone secretion, paralleled by the decrease in interaction between CREB and CRTC2, and the binding of CREB/CRTC2 complex to the StAR promoter region. Furthermore, inhibition of p38 MAPK or PKA signaling pathway can significantly alleviate the above PFOS-induced effects in Leydig cells. Taken together, these data strongly suggest that CREB/CRTC2/StAR signaling pathway contributes to the PFOS-induced suppression of testosterone biosynthesis.

5. Conclusion

In summary, the present results demonstrate that exposure to PFOS activates PKA, p38 MAPK and CREB, and decreases CRTC2 expression, which subsequently affects the interaction between CREB and CRTC2, and CREB/CRTC2 complex binding to the StAR promoter region, resulting in the downregulating of StAR gene and the suppression of testosterone biosynthesis (Fig. 8). Therefore, the CREB/CRTC2/StAR signaling pathway may play an important role in PFOS-induced suppression of testosterone biosynthesis, contributing to the PFOS-induced male reproductive disorder.

Declaration of Competing Interest

The authors report no declarations of interest.

Acknowledgements

This work was supported by National Natural Science Foundation of China (No. 81302452), Major Projects of Natural Sciences of University in Jiangsu Province of China (18KJB330004), a project fund of Basic Scientific Research program of Nantong City (JC2019021) and Scientific Research Starting Foundation for The Doctoral researcher of Nantong University (No. 14B14).

References

- Altarejos, J.Y., Montminy, M., 2011. CREB and the CRTC co-activators: sensors for hormonal and metabolic signals. *Nat. Rev. Mol. Cell Biol.* 12, 141–151.
- Ballesteros, V., Costa, O., Iniguez, C., Fletcher, T., Ballester, F., Lopez-Espinosa, M.J., 2017. Exposure to perfluoroalkyl substances and thyroid function in pregnant women and children: a systematic review of epidemiologic studies. *Environ. Int.* 99, 15–28.
- Berntsen, H.F., Moldes-Anaya, A., Bjorklund, C.G., Ragazzi, L., Haug, T.M., Strandabo, R. A.U., Verhaegen, S., Paulsen, R.E., Ropstad, E., Tasker, R.A., 2020. Perfluoroalkyl acids potentiate glutamate excitotoxicity in rat cerebellar granule neurons. *Toxicology* 445, 152610.
- Delghandi, M.P., Johannessen, M., Moens, U., 2005. The cAMP signalling pathway activates CREB through PKA, p38 and MSK1 in NIH 3T3 cells. *Cell. Signal.* 17, 1343–1351.
- Dong, G.H., Zhang, Y.H., Zheng, L., Liu, W., Jin, Y.H., He, Q.C., 2009. Chronic effects of perfluorooctanesulfonate exposure on immunotoxicity in adult male C57BL/6 mice. *Arch. Toxicol.* 83, 805–815.
- Gao, T., Lin, M., Shao, B., Zhou, Q., Wang, Y., Chen, X., Zhao, D., Dai, X., Shen, C., Cheng, H., Yang, S., Li, H., Zheng, B., Zhong, X., Yu, J., Chen, L., Huang, X., 2020. BMI1 promotes steroidogenesis through maintaining redox homeostasis in mouse MLTC-1 and primary Leydig cells. *Cell Cycle* 19, 1884–1898.
- Huang, Y., Zhu, J., Li, H., Wang, W., Li, Y., Yang, X., Zheng, N., Liu, Q., Zhang, Q., Zhang, W., Liu, J., 2020. Cadmium exposure during prenatal development causes testosterone disruption in multigeneration via SF-1 signaling in rats. *Food Chem. Toxicol.* 135, 110897.
- Jian, J.M., Guo, Y., Zeng, L., Liang-Ying, L., Lu, X., Wang, F., Zeng, E.Y., 2017. Global distribution of perfluorochemicals (PFCS) in potential human exposure source—a review. *Environ. Int.* 108, 51–62.
- Joensen, U.N., Veyrand, B., Antignac, J.P., Blomberg Jensen, M., Petersen, J.H., Marchand, P., Skakkebaek, N.E., Andersson, A.M., Le Bizec, B., Jorgensen, N., 2013. PFOS (perfluorooctanesulfonate) in serum is negatively associated with testosterone levels, but not with semen quality, in healthy men. *Hum. Reprod.* 28, 599–608.
- Lai, W.A., Yeh, Y.T., Fang, W.L., Wu, L.S., Harada, N., Wang, P.H., Ke, F.C., Lee, W.L., Hwang, J.J., 2014. Calcineurin and CRTC2 mediate FSH and TGFbeta1 upregulation of Cyp19a1 and Nr5a in ovary granulosa cells. *J. Mol. Endocrinol.* 53, 259–270.
- Lau, C., Thibodeaux, J.R., Hanson, R.G., Rogers, J.M., Grey, B.E., Stanton, M.E., Butenhoff, J.L., Stevenson, L.A., 2003. Exposure to perfluorooctane sulfonate during pregnancy in rat and mouse. II: postnatal evaluation. *Toxicol. Sci.* 74, 382–392.

- Lee, J., Tong, T., Takemori, H., Jefcoate, C., 2015. Stimulation of STAR expression by cAMP is controlled by inhibition of highly inducible SIK1 via CRT2, a co-activator of CREB. *Mol. Cell. Endocrinol.* 408, 80–89.
- Li, W., He, Q.Z., Wu, C.Q., Pan, X.Y., Wang, J., Tan, Y., Shan, X.Y., Zeng, H.C., 2015. PFOS disturbs BDNF-ERK-CREB signalling in association with increased MicroRNA-22 in SH-SY5Y cells. *Biomed Res. Int.* 2015, 302653.
- Li, L., Li, X., Chen, X., Chen, Y., Liu, J., Chen, F., Ge, F., Ye, L., Lian, Q., Ge, R.S., 2018a. Perfluorooctane sulfonate impairs rat Leydig cell development during puberty. *Chemosphere* 190, 43–53.
- Li, R., Xin, T., Li, D., Wang, C., Zhu, H., Zhou, H., 2018b. Therapeutic effect of Sirtuin 3 on ameliorating nonalcoholic fatty liver disease: the role of the ERK-CREB pathway and Bnip3-mediated mitophagy. *Redox Biol.* 18, 229–243.
- Lindstrom, A.B., Strynar, M.J., Libelo, E.L., 2011. Polyfluorinated compounds: past, present, and future. *Environ. Sci. Technol.* 45, 7954–7961.
- Liu, D., Liu, N.Y., Chen, L.T., Shao, Y., Shi, X.M., Zhu, D.Y., 2020a. Perfluorooctane sulfonate induced toxicity in embryonic stem cell-derived cardiomyocytes via inhibiting autophagy-lysosome pathway. *Toxicol. In Vitro* 69, 104988.
- Liu, Y., Li, A., Buchanan, S., Liu, W., 2020b. Exposure characteristics for congeners, isomers, and enantiomers of perfluoroalkyl substances in mothers and infants. *Environ. Int.* 144, 106012.
- Lopez-Doval, S., Salgado, R., Pereiro, N., Moyano, R., Lafuente, A., 2014. Perfluorooctane sulfonate effects on the reproductive axis in adult male rats. *Environ. Res.* 134, 158–168.
- Moon, M.K., Kang, G.H., Kim, H.H., Han, S.K., Koo, Y.D., Cho, S.W., Kim, Y.A., Oh, B.C., Park, D.J., Chung, S.S., Park, K.S., Park, Y.J., 2016. Thyroid-stimulating hormone improves insulin sensitivity in skeletal muscle cells via cAMP/PKA/CREB pathway-dependent upregulation of insulin receptor substrate-1 expression. *Mol. Cell. Endocrinol.* 436, 50–58.
- Mshaty, A., Hajjima, A., Takatsuru, Y., Ninomiya, A., Yajima, H., Kokubo, M., Khairinisa, M.A., Miyazaki, W., Amano, I., Koibuchi, N., 2020. Neurotoxic effects of lactational exposure to perfluorooctane sulfonate on learning and memory in adult male mouse. *Food Chem. Toxicol.* 111710.
- Olsen, G.W., Burris, J.M., Ehresman, D.J., Froehlich, J.W., Seacat, A.M., Butenhoff, J.L., Zobel, L.R., 2007. Half-life of serum elimination of perfluorooctanesulfonate, perfluorohexanesulfonate, and perfluorooctanoate in retired fluorochemical production workers. *Environ. Health Perspect.* 115, 1298–1305.
- Pan, Y., Cui, Q., Wang, J., Sheng, N., Jing, J., Yao, B., Dai, J., 2019. Profiles of emerging and legacy per-/polyfluoroalkyl substances in matched serum and semen samples: new implications for human semen quality. *Environ. Health Perspect.* 127, 127005.
- Pham, A., Zhang, J., Feng, L., 2020. Exposure to perfluorobutane sulfonate and perfluorooctanesulfonic acid disrupts the production of angiogenesis factors and stress responses in human placental syncytiotrophoblast. *Reprod. Toxicol.*
- Pierozan, P., Cattani, D., Karlsson, O., 2020. Perfluorooctane sulfonate (PFOS) and perfluorooctanoic acid (PFOA) induce epigenetic alterations and promote human breast cell carcinogenesis in vitro. *Arch. Toxicol.* 94, 3893–3906.
- Qiu, L., Qian, Y., Liu, Z., Wang, C., Qu, J., Wang, X., Wang, S., 2016. Perfluorooctane sulfonate (PFOS) disrupts blood-testis barrier by down-regulating junction proteins via p38 MAPK/ATF2/MMP9 signaling pathway. *Toxicology* 373, 1–12.
- Qiu, L., Chen, M., Wang, X., Qin, X., Chen, S., Qian, Y., Liu, Z., Cao, Q., Ying, Z., 2018. Exposure to concentrated ambient PM2.5 compromises spermatogenesis in a mouse model: role of suppression of hypothalamus-pituitary-gonads axis. *Toxicol. Sci.* 162, 318–326.
- Salas-Huetos, A., Maghsoumi-Norouzabad, L., James, E.R., Carrell, D.T., Aston, K.I., Jenkins, T.G., Becerra-Tomas, N., Javid, A.Z., Abed, R., Torres, P.J., Luque, E.M., Ramirez, N.D., Martini, A.C., Salas-Salvado, J., 2020. Male adiposity, sperm parameters and reproductive hormones: an updated systematic review and collaborative meta-analysis. *Obes. Rev.*
- Sifakis, S., Androutsopoulos, V.P., Tsatsakis, A.M., Spandidos, D.A., 2017. Human exposure to endocrine disrupting chemicals: effects on the male and female reproductive systems. *Environ. Toxicol. Pharmacol.* 51, 56–70.
- Stratakis, N., Conti, D.V., Jin, R., Margetaki, K., Valvi, D., Siskos, A.P., Maitre, L., Garcia, E., Varo, N., Zhao, Y., Roumeliotaki, T., Vafeiadi, M., Urquiza, J., Fernandez-Barres, S., Heude, B., Basagana, X., Casas, M., Fossati, S., Grazuleviciene, R., Andrusaityte, S., Uppal, K., McEachan, R.R., Papadopoulou, E., Robinson, O., Haug, L.S., Wright, J., Vos, M.B., Keun, H.C., Vrijheid, M., Berhane, K.T., McConnell, R., Chatzi, L., 2020. Prenatal exposure to perfluoroalkyl substances associated with increased susceptibility to liver injury in children. *Hepatology.*
- Tout, I., Gomes, M., Ainouze, M., Marotel, M., Pecoul, T., Durantel, D., Vaccarella, S., Dubois, B., Loustaud-Ratti, V., Walzer, T., Alain, S., Chemin, I., Hasan, U., 2018. Hepatitis B virus blocks the CRE/CREB complex and prevents TLR9 transcription and function in human B cells. *J. Immunol.* 201, 2331–2344.
- Tugaeva, K.V., Sluchanko, N.N., 2019. Steroidogenic acute regulatory protein: structure, functioning, and regulation. *Biochem. (Mosc.)* 84, S233–S253.
- UNEP, 2009. Listing of Perfluorooctane Sulfonic Acid, Its Salts and Perfluorooctane Sulfonyl Fluoride. UNEP/POPS/COP.4/SC.4/17 (2009). UNEP.
- Wan, H.T., Zhao, Y.G., Wong, M.H., Lee, K.F., Yeung, W.S., Giesy, J.P., Wong, C.K., 2011. Testicular signaling is the potential target of perfluorooctanesulfonate-mediated subfertility in male mice. *Biol. Reprod.* 84, 1016–1023.
- Wan, H.T., Lai, K.P., Wong, C.K., 2020. Comparative analysis of PFOS and PFOA toxicity on sertoli cells. *Environ. Sci. Technol.* 54, 3465–3475.
- Wang, T., Wang, P., Meng, J., Liu, S., Lu, Y., Khim, J.S., Giesy, J.P., 2015. A review of sources, multimedia distribution and health risks of perfluoroalkyl acids (PFAAs) in China. *Chemosphere* 129, 87–99.
- Xia, Y., Yang, X., Lu, J., Xie, Q., Ye, A., Sun, W., 2020. The endoplasmic reticulum stress and related signal pathway mediated the glyphosate-induced testosterone synthesis inhibition in TM3 cells. *Environ. Pollut.* 260, 113949.
- Xing, J., Wang, G., Zhao, J., Wang, E., Yin, B., Fang, D., Zhao, J., Zhang, H., Chen, Y.Q., Chen, W., 2016. Toxicity assessment of perfluorooctane sulfonate using acute and subchronic male C57BL/6J mouse models. *Environ. Pollut.* 210, 388–396.
- Xu, J.N., Zeng, C., Zhou, Y., Peng, C., Zhou, Y.F., Xue, Q., 2014. Metformin inhibits StAR expression in human endometrial stromal cells via AMPK-mediated disruption of CREB-CRTC2 complex formation. *J. Clin. Endocrinol. Metab.* 99, 2795–2803.
- Yu, W.G., Liu, W., Jin, Y.H., 2009. Effects of perfluorooctane sulfonate on rat thyroid hormone biosynthesis and metabolism. *Environ. Toxicol. Chem./SETAC* 28, 990–996.
- Yu, W.G., Liu, W., Liu, L., Jin, Y.H., 2011. Perfluorooctane sulfonate increased hepatic expression of OAPT2 and MRP2 in rats. *Arch. Toxicol.* 85, 613–621.
- Zhou, R., Wu, J., Liu, B., Jiang, Y., Chen, W., Li, J., He, Q., He, Z., 2019. The roles and mechanisms of Leydig cells and myoid cells in regulating spermatogenesis. *Cell. Mol. Life Sci.* 76, 2681–2695.
- Zirkin, B.R., Papadopoulos, V., 2018. Leydig cells: formation, function, and regulation. *Biol. Reprod.* 99, 101–111.